Dynamics of a two-level system coupled to a bath of spins

Cite as: J. Chem. Phys. **137**, 22A504 (2012); https://doi.org/10.1063/1.4732808
Submitted: 03 May 2012 . Accepted: 19 June 2012 . Published Online: 13 July 2012

Haobin Wang, and Jiushu Shao

Dynamics of a two-level system coupled to a bath of spins

Haobin Wang[1] and Jiushu Shao[2]
[1]*Department of Chemistry and Biochemistry, MSC 3C, New Mexico State University, Las Cruces, New Mexico 88003, USA and Beijing Computational Science Research Center, No. 3 He-Qing Road, Hai-Dian District, Beijing 100084, People's Republic of China*
[2]*College of Chemistry and Key Laboratory of Theoretical and Computational Photochemistry, Ministry of Education, Beijing Normal University, Beijing 100875, People's Republic of China*

(Received 3 May 2012; accepted 19 June 2012; published online 13 July 2012)

The dynamics of a two-level system coupled to a spin bath is investigated via the numerically exact multilayer multiconfiguration time-dependent Hartree (ML-MCTDH) theory. Consistent with the previous work on linear response approximation [N. Makri, J. Phys. Chem. B **103**, 2823 (1999)], it is demonstrated numerically that this spin-spin-bath model can be mapped onto the well-known spin-boson model if the system-bath coupling strength obeys an appropriate scaling behavior. This linear response mapping, however, may require many bath spin degrees of freedom to represent the practical continuum limit. To clarify the discrepancies resulted from different approximate treatments of this model, the population dynamics of the central two-level system has been investigated near the transition boundary between the coherent and incoherent motions via the ML-MCTDH method. It is found that increasing temperature favors quantum coherence in the nonadiabatic limit of this model, which corroborates the prediction in the previous work [J. Shao and P. Hanggi, Phys. Rev. Lett. **81**, 5710 (1998)] based on the non-interacting blip approximation (NIBA). However, the coherent-incoherent boundary obtained by the exact ML-MCTDH simulation is slightly different from the approximate NIBA results. Quantum dynamics in other physical regimes are also discussed.
 [http://dx.doi.org/10.1063/1.4732808]

I. INTRODUCTION

Understanding quantum dynamics in condensed phases is an important and challenging topic in modern theoretical chemistry and physics. Although in general the environment is dissipative, quantum coherence may survive to a relatively long time as suggested by recent time-resolved optical experiments. The detailed description of the dissipative dynamics has been based on the system-plus-bath model from which the reduced density operator fully characterizes the dynamics of the dissipative system. Usually the size of the total system *à la* system-plus-bath is very large, which makes it difficult if not impossible to construct reliable many-body potential energy surfaces from first-principles calculations. Instead, simpler models are proposed to capture the essential physics of the problem, for example, force fields in molecular dynamics simulations, models based on linear response approximation, and so on. Among these the most popular approach is the Caldeira-Leggett model[1,2] in which the bath consists of an ensemble of harmonic oscillators with linear couplings to the system. This model has been widely used in condensed phase physics and chemistry to represent a variety of different dissipative processes. An interesting example is the spin-boson Hamiltonian[3,4] where a system of two states is linearly coupled to a bath of harmonic oscillators. In mass-weighted coordinates, the Hamiltonian has the form (in this paper atomic units are used where $\hbar = 1$)

$$H = \epsilon\sigma_z + \Delta\sigma_x + \frac{1}{2}\sum_i \left(p_i^2 + \omega_i^2 q_i^2\right) + \sigma_z \sum_i c_i q_i, \quad (1.1)$$

where ϵ is the energy bias for the two-level subsystem, Δ is the nonadiabatic coupling, and σ_x and σ_z are Pauli matrices

$$\sigma_x = |\phi_1\rangle\langle\phi_2| + |\phi_2\rangle\langle\phi_1|, \quad (1.2a)$$

$$\sigma_z = |\phi_1\rangle\langle\phi_1| - |\phi_2\rangle\langle\phi_2|, \quad (1.2b)$$

with $|\phi_1\rangle$ and $|\phi_2\rangle$ representing two localized states. Within the linear response framework the properties of the bath that influence the dynamics of the two-state subsystem are completely specified by the spectral density function[3,4]

$$J_B(\omega) = \frac{\pi}{2}\sum_j \frac{c_j^2}{\omega_j}\delta(\omega - \omega_j). \quad (1.3)$$

Despite its simple form, the spin-boson model is not analytically solvable and in fact quite challenging in some strong coupling regimes. It is the subject of various approximate[3–19] and numerically exact[20–31] treatment and has been used to model a variety of different processes such as electron transfer,[32] hydrogen tunneling,[33] macroscopic quantum coherence,[34] and many others.[4]

The harmonic boson bath is often considered to be a model for collective variables near equilibrium. If one considers another type of media, e.g., a spin glass or an array of nuclear spins in electronic or magnetic materials, a spin bath model[35,36] seems to be a logical choice. The resulting spin-spin-bath model can be written in a similar form to Eq. (1.1)

$$H = \epsilon\sigma_z + \Delta\sigma_x + \frac{1}{2}\sum_i \omega_i s_z^i + \sigma_z \sum_i \frac{c_i}{\sqrt{2\omega_i}} s_x^i, \quad (1.4)$$

where s_z^i and s_x^i are Pauli matrices for the ith mode of the spin bath. Put differently, the spin bath can be regarded as a truncated bosonic bath in Eq. (1.1) in which each harmonic oscillator is confined to only two eigenstates. The fact that only single excitation is allowed for each bath spin seems to suggest that quite different physics may be expected between this spin-spin-bath model and the well-known spin-boson model. Indeed, using the resolvent operator approach, Shao and Hänggi[37] found that by increasing the temperature of the spin bath the coherence of the central two-level subsystem is actually enhanced rather than suppressed, which contradicts the conventional wisdom that a heat bath usually causes dissipative and decoherence dynamics to the subsystem it is connected to. A subsequent study,[38] employing the non-interacting blip approximation (NIBA) (Ref. 3) gauged by the numerical path integral simulation, support this finding that the coherent-incoherent boundary is shifted to the stronger coupling regime upon increasing the temperature. However, there appears to be some disagreement on this conclusion as well as the exact location of the phase boundary with respect to the temperature and the coupling strength (*vide infra*). This was discussed in a more recent publication[39] using a perturbation approach based on a polaron-like transformation technique. A major finding of the paper is that the coherent-incoherent boundary is independent of the bath temperature, which is different from the results discussed above.

The qualitatively different conclusions drawn from each work depend largely on the specific perturbational approach employed, and it is difficult to check the validity of the perturbation theory without prior knowledge on the exact (quantitative) physics of the relevant problem. Therefore, we have carried out numerically exact quantum dynamics study on the spin-spin-bath model using the multilayer multiconfiguration time-dependent Hartree (ML-MCTDH) theory.[40] In particular, we are interested in physical regimes that are difficult to be treated by approximate perturbation theories, e.g., stronger couplings and/or lower temperatures. Furthermore, we are interested in understanding the underlying physics between coherent to incoherent transitions in the spin-spin-bath model and the different impact between the spin and the boson bath on the reduced dynamics of the central two-level subsystem.

To facilitate such an analysis on the current model, one of the most useful tools is the linear response mapping of the environment to an effective harmonic bath.[1,2,33,41] In general, linear response is an approximation that only takes into account the second order contribution of the interaction with the environment. However, if the system-bath coupling is distributed uniformly over all the bath degrees of freedom, it is shown that linear response is exact if the bath is (practically) infinitely large.[33,41] In this case the influence functional has a Gaussian form and the overall two-level/bath model can be mapped onto the form of the spin-boson Hamiltonian with an effective spectral density.[33,41] The harmonic form for the effective bath does not imply that the microscopic potentials of the environment are quadratic. Rather, it is a mapping in the context of the linear response limit whose parameters are defined in such a way that its force-force correlation function at a certain temperature agrees with that of the original environment.[33,41,42] The actual nuclear potential energy function may be quite anharmonic,[42] which renders a local harmonic approximation invalid. Sometimes, the analysis of such an effective harmonic bath model is crucial for obtaining an approximate picture of the spin-spin-bath model at various temperatures, although in this work our simulation also reveals some counter-intuitive features that are subtle for a simple qualitative interpretation.

The remainder of the paper is as follows. In Sec. II we outline the physical model and the quantum ML-MCTDH method used in our study. In Sec. III, we first present numerical results to investigate the linear response limit of the spin-spin model and its practical realization. This is followed by the study of the coherent to incoherent transition versus the system-bath coupling strength, particularly in the low temperature regimes. Section IV summarizes our findings.

II. THEORETICAL METHODOLOGY

A. Model and observable of interest

The spin-spin-bath Hamiltonian of Eq. (1.4) is employed in our study. Similar to the previous work[37–39] we consider a symmetric two-level subsystem ($\epsilon = 0$) and assume that the spin bath and its coupling to the central two levels can be characterized by a continuous spectral density function, here an Ohmic form with an exponential cutoff

$$J(\omega) = \frac{\pi}{2}\alpha\omega\, e^{-\omega/\omega_c}. \tag{2.1}$$

In this expression, α is the dimensionless Kondo parameter that characterizes the system-bath coupling strength and ω_c is the cutoff frequency/energy-splitting of the bath. The Ohmic spectral density is often found in the study of the spin-boson model described by Eq. (1.1). A discretization of the continuous spectral density function in the form of (1.3) can be achieved via the relation[29,30,40]

$$c_j^2 = \frac{2}{\pi}\omega_j \frac{J(\omega_j)}{\rho(\omega_j)}, \tag{2.2a}$$

where $\rho(\omega)$ is a density of frequencies satisfying

$$\int_0^{\omega_j} d\omega\, \rho(\omega) = j, \quad j = 1, \ldots, N_b, \tag{2.2b}$$

and N_b is the number of bath modes.

The functional form for $\rho(\omega)$ is arbitrary as long as it covers the whole spectral range and ensures $c_j^2 \sim 1/N_b$ as $N_b \to \infty$. For practical purpose an appropriate choice of $\rho(\omega)$ can make the simulation more effective by requiring less number of modes to converge. In this work, $\rho(\omega)$ is chosen as

$$\rho(\omega) = \frac{N_b + 1}{\omega_c} e^{-\omega/\omega_c}. \tag{2.3}$$

The specific number of bath modes depends on the time scale of interest and the system-bath coupling strength. To ensure convergence to the condensed phase limit, we have employed a few hundred to ten thousand spin modes for the various cases discussed in this paper.

To improve the efficiency of the calculations, some of the high-frequency spin modes can be removed from the dynamical simulation using a Born-Oppenheimer type

approximation,[3] resulting in a modified electronic coupling

$$\Delta_{\rm eff} = \Delta \exp\left[-\frac{2}{\pi}\int_{\omega_q}^{\infty} d\omega \frac{J(\omega)}{\omega^2}\right]. \tag{2.4}$$

Here, ω_q defines the boundary frequency above which the modes are not treated explicitly in the dynamical simulation but are included via the effective coupling parameter $\Delta_{\rm eff}$. It is thus a numerical convergence parameter. It should be stressed that the sole purpose of using Eq. (2.4) to remove high-frequency modes is to accelerate the calculations. The ML-MCTDH method does not rely on this trick and can handle all the bath modes in the simulation (albeit at a higher computational but tractable cost.) One advantage of performing this reduction is to investigate to what extent the high-frequency modes is irrelevant to the reduced dynamics of the two-level subsystem thus providing insights into the development of approximate theories. It is found that this reduction is only useful for low bath temperatures and/or weak system-bath couplings.

In this paper, the observable of interest is the time-dependent population difference of the two localized states $|\phi_1\rangle$ and $|\phi_2\rangle$,

$$P(t) \equiv \langle\sigma_z(t)\rangle = \frac{1}{{\rm tr}[e^{-\beta H_B}]}{\rm tr}[e^{-\beta H_B}|\phi_1\rangle\langle\phi_1|\, e^{iHt}\sigma_z e^{-iHt}], \tag{2.5}$$

where we consider a factorized initial state specified by the density operator $|\phi_1\rangle\langle\phi_1|$ for the central spin and the equilibrium Boltzmann operator $e^{-\beta H_B}/{\rm tr}(e^{-\beta H_B})$ for the bath. The Hamiltonian of the bath, H_B, is given by

$$H_B = \frac{1}{2}\sum_i \omega_i s_z^i. \tag{2.6}$$

To evaluate the trace at a certain temperature ($\beta = 1/k_B T$) we use a direct product basis $|\mathbf{n}\rangle|\phi_1\rangle$ such that

$$e^{-\beta H_B} = \sum_{\mathbf{n}} e^{-\beta E_{\mathbf{n}}}|\mathbf{n}\rangle\langle\mathbf{n}|, \tag{2.7}$$

where the bath state $\{|\mathbf{n}\rangle\} \equiv \{|n_1\rangle|n_2\rangle\ldots|n_{N_b}\rangle\}$ is a direct product of the bath spin states with the occupation n_i of each mode selected via a Monte Carlo importance sampling technique.[40,43,44] The trace in Eq. (2.5) is then written as

$$P(t) = \frac{1}{\sum_{\mathbf{n}} e^{-\beta E_{\mathbf{n}}}}\sum_{\mathbf{n}} e^{-\beta E_{\mathbf{n}}}\langle\Psi_{\mathbf{n}}(t)|\sigma_z|\Psi_{\mathbf{n}}(t)\rangle, \tag{2.8a}$$

where

$$|\Psi_{\mathbf{n}}(t)\rangle = e^{-iHt}|\Psi_{\mathbf{n}}(0)\rangle = e^{-iHt}|\phi_1\rangle|\mathbf{n}\rangle. \tag{2.8b}$$

The time propagation of each wave function can be carried out using the ML-MCTDH method.

B. Multilayer multiconfiguration time-dependent Hartree theory

To obtain the time-dependent population difference $P(t)$ in Eqs. (2.8a) and (2.8b), the current approach requires the time-dependent wave function $e^{-iHt}|\Psi_0\rangle$. This is achieved by employing the ML-MCTDH theory.[40] This method generalizes the original MCTDH method[45–48] for applications to significantly larger systems and has been applied extensively to reactions in the condensed phase.[40,42,43,49–60]

Briefly speaking, the ML-MCTDH method[40] is a rigorous variational approach to study quantum dynamics in systems with many degrees of freedom. Within this approach the time-dependent wave function is expressed by a recursive, layered expansion

$$|\Psi(t)\rangle = \sum_{j_1}\sum_{j_2}\cdots\sum_{j_p} A_{j_1 j_2\ldots j_p}(t)\prod_{\kappa=1}^{p}\left|\varphi_{j_\kappa}^{(\kappa)}(t)\right\rangle, \tag{2.9a}$$

$$\left|\varphi_{j_\kappa}^{(\kappa)}(t)\right\rangle = \sum_{i_1}\sum_{i_2}\cdots\sum_{i_{Q(\kappa)}} B_{i_1 i_2\ldots i_{Q(\kappa)}}^{\kappa,j_\kappa}(t)\prod_{q=1}^{Q(\kappa)}\left|v_{i_q}^{(\kappa,q)}(t)\right\rangle, \tag{2.9b}$$

$$\left|v_{i_q}^{(\kappa,q)}(t)\right\rangle = \sum_{\alpha_1}\sum_{\alpha_2}\cdots\sum_{\alpha_{M(\kappa,q)}} C_{\alpha_1\alpha_2\ldots\alpha_{M(\kappa,q)}}^{\kappa,q,i_q}(t)\prod_{\gamma=1}^{M(\kappa,q)}\left|\xi_{\alpha_\gamma}^{\kappa,q,\gamma}(t)\right\rangle, \tag{2.9c}$$

$$\ldots$$

where $A_{j_1 j_2\ldots j_p}(t)$, $B_{i_1 i_2\ldots i_{Q(\kappa)}}^{\kappa,j_\kappa}(t)$, $C_{\alpha_1\alpha_2\ldots\alpha_{M(\kappa,q)}}^{\kappa,q,i_q}(t)$, and so on are the expansion coefficients for the first, second, third, ..., layers, respectively; $|\varphi_{j_\kappa}^{(\kappa)}(t)\rangle$, $|v_{i_q}^{(\kappa,q)}(t)\rangle$, $|\xi_{\alpha_\gamma}^{\kappa,q,\gamma}(t)\rangle$, ..., are the single particle functions (SPFs) for the first, second, third, ..., layers. The notations beyond the first layer are as follows. In Eq. (2.9b) $Q(\kappa)$ is the number of (level 2) single particle (SP) groups for the second layer that belongs to the κth (level 1) SP group in the first layer, i.e., there are a total of $\sum_{\kappa=1}^{p} Q(\kappa)$ second layer SP groups. Continuing along the multilayer hierarchy, $M(\kappa, q)$ in Eq. (2.9c) is the number of (level 3) SP groups for the third layer that belongs to the qth (level 2) SP group of the second layer and the κth (level 1) SP group of the first layer, resulting in a total of $\sum_{\kappa=1}^{p}\sum_{q=1}^{Q(\kappa)} M(\kappa, q)$ third layer SP groups. Such a recursive expansion can be carried out to an arbitrary number of layers. To terminate the multilayer hierarchy at a particular level, the SPFs in the deepest layer are expanded in terms of time-independent configurations. For example, in the four-layer version of the ML-MCTDH theory, the fourth layer is expanded in the time-independent basis functions/configurations, each of which may still contain several degrees of freedom.

Applying the Dirac-Frenkel variational principle, $\langle\delta\Psi(t)|i\frac{\partial}{\partial t} - \hat{H}|\Psi(t)\rangle = 0$, with the functional form in Eqs. (2.9a)–(2.9c), the coupled equations of motion can be obtained[40,56] for the time derivatives of expansion coefficients of all the layers. For a N-layer version, there are $N + 1$ levels of expansion coefficients because the SPFs in the deepest layer need to be expanded in time-independent basis functions/configurations. In this sense the conventional wave packet propagation method is a "zero-layer" MCTDH approach. The introduction of this recursive, dynamically optimized layering scheme in the ML-MCTDH wavefunction provides much more flexibility in the variational functional, which significantly advances the capabilities of performing wave packet propagations for large systems.[40,42,43,49–60] In

this work, we employ an implementation of the ML-MCTDH theory with up to four dynamical layers. Without specified otherwise, only converged results are shown.

III. RESULTS AND DISCUSSION

A. The practical linear response limit

The fact that we assume a continuous spectral density function (2.1) for the spin bath already implies that the model satisfies the linear response requirement. This can be understood from the discretization scheme described in Eqs. (2.2a) and (2.2b), which possesses two basic properties: (1) the coupling parameter c_j can be made arbitrarily small once the number of bath modes N_b becomes arbitrarily large, thus in an average sense the system-bath coupling is distributed uniformly over all the bath degrees of freedom; (2) the coupling follows the general scaling behavior $c_j^2 \sim 1/N_b$ in the $N_b \to \infty$ limit. Under these conditions and based on the work of Suarez and Silbey,[33] Makri[41] has shown that only the second order term retains in the cumulant expansion of the influence functional for $N_b \to \infty$. That is, the linear response mapping is exact in the infinite bath modes limit and the spin-spin-bath model can be mapped onto the familiar spin-boson model, for which the effective spectral density of the harmonic bath is[36]

$$J_{\text{eff}}(\omega, \beta) = \tanh(\beta\omega/2) J(\omega). \tag{3.1}$$

In particular, $J_{\text{eff}}(\omega, \beta)$ is the same as $J(\omega)$ at zero temperature. In this limit, the spin-spin-bath and the spin-boson model have the same reduced dynamics for the central two-level subsystem.

For realistic applications the system-bath type models are often derived from large but finite systems according to, e.g., molecular dynamics simulations or first-principles calculations. In this situation the linear response mapping is only approximate. It is thus useful to investigate the practical condition under which linear response holds. To map the current spin-spin bath model onto the linear response spin-boson model, one needs to ensure that enough number of spin modes are included so that the system-bath coupling is diluted over many of them. For higher temperatures only a moderate number of bath spin modes (less than a few hundred) are required to achieve numerical convergence.[41] This will not be the case for lower temperatures and/or stronger system-bath couplings. Below, we present results for the most quantum regime, the zero temperature for the bath. Since in this limit the spin-spin-bath and the spin-boson model have the same reduced dynamics, converged results can be obtained from the latter model using the same ML-MCTDH approach described previously.[55,58]

Figure 1 shows results for a regime that the system and bath have similar time scales, $\omega_c/\Delta = 1$. For a weaker coupling strength in Fig. 1(a), $\alpha = 0.5$, pronounced coherence is found in $P(t)$ defined in Eq. (2.5). It is seen that 100 bath spins already provide a reasonable description of the dynamics within the time scale shown in the plot, although there are small recurrences at longer times. In this case, the linear response limit is numerically achieved (within the time scale

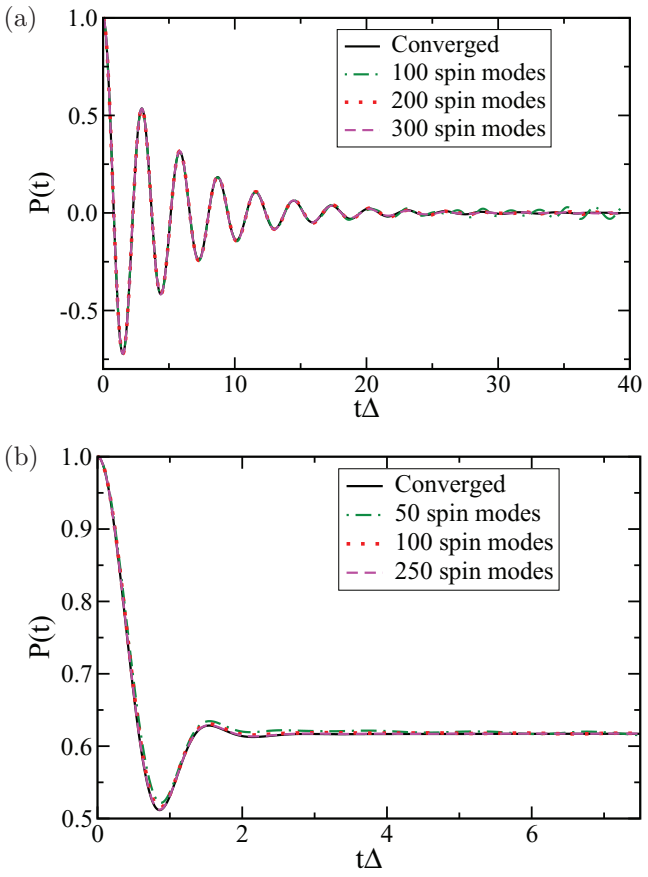

FIG. 1. Time-dependent population difference, Eq. (2.8), for a spin bath with a characteristic frequency $\omega_c/\Delta = 1$ and zero temperature. The Kondo parameters are: (a) $\alpha = 0.5$, (b) $\alpha = 10$.

depicted in the graph) with 200–300 bath spin modes. Similar findings are obtained for a stronger coupling in Fig. 1(b) with a Kondo parameter $\alpha = 10$, where localization in the central two-level's population is found after a transient coherent period. This is typical when the time scale of the bath is similar to or longer than that of the subsystem.[58] Compared with Fig. 1(a), the time scale for $P(t)$ to reach its stationary value is shorter. To study relevant dynamics of the model, one is usually only interested in such a time scale. For this purpose a few hundred spin modes are satisfactory. For comparison, the converged results are obtained for the corresponding spin-boson model with less than 300 bath modes.

Thus, for a relatively narrow spectral density such as the Ohmic form with an exponential cutoff, only a moderate number of bath modes are required to fulfill the linear response requirement if there is a match between the time scales of the bath and the system. This is because within the limited spectral range all the discrete bath modes are coupled to the subsystem at roughly the same scale, which effectively dilutes the system-bath coupling strength. This is not true if the spectral density covers a broader range of frequencies such as in a glassy environment. Even for the current spectral density, in the adiabatic or the nonadiabatic regime there is a mismatch of the time scale between the bath and the system, which renders less effective coupling of each individual mode. At zero temperature the reduced dynamics for the former is usually characterized by a coherent motion in the weak coupling

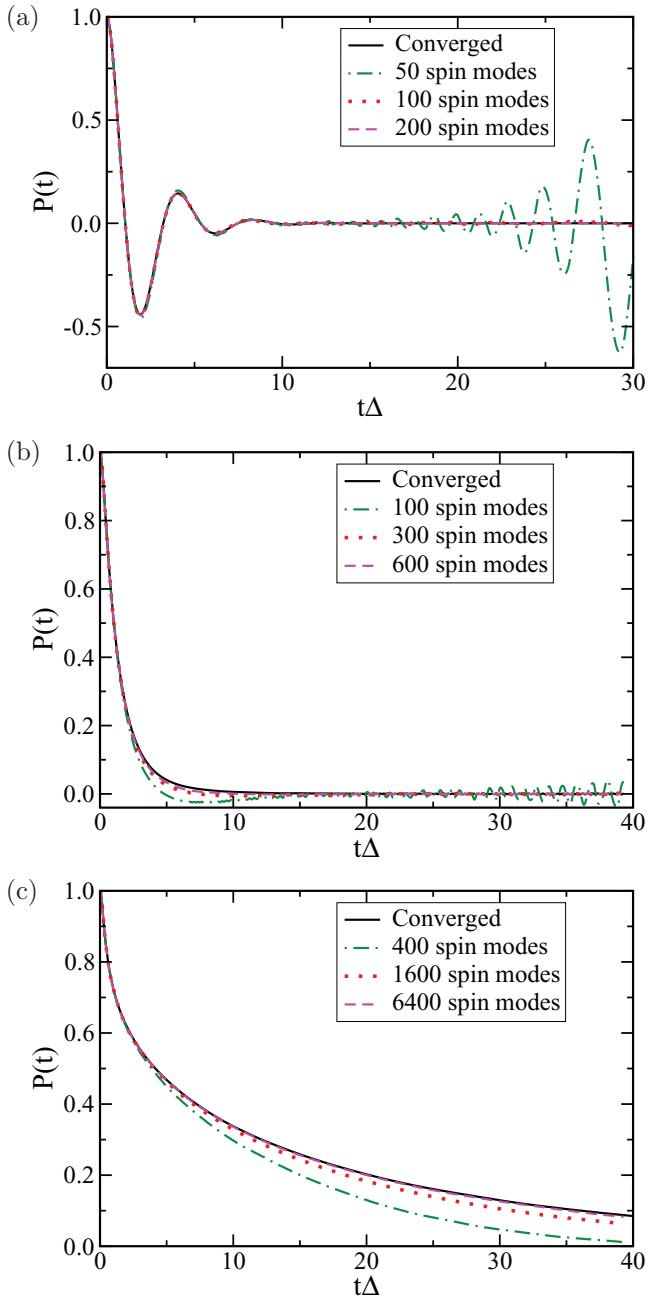

FIG. 2. Time-dependent population difference for a spin bath with a characteristic frequency $\omega_c/\Delta = 10$ and zero temperature. The Kondo parameters are: (a) $\alpha = 0.2$, (b) $\alpha = 0.5$, (c) $\alpha = 0.75$.

regime and localization in the strong coupling limit, whereas for the latter it shows a coherent to incoherent transition which is more relevant to the topic discussed in this paper and will be presented below.

Figure 2 shows $P(t)$ in a nonadiabatic regime, $\omega_c/\Delta = 10$, for different values of the system-bath coupling strength. The characteristics of the population dynamics change from weakly damped coherent oscillation to incoherent decay when the Kondo parameter α increases from 0.2 to 0.75. For a weaker coupling strength in Fig. 2(a) the dynamics is converged with 200 bath spin modes. At a moderate coupling strength, $\alpha = 0.5$, there is a small negative lobe in $P(t)$ obtained with the 300 spin modes that is absent from the converged result. Thus, at least 600 spin modes are needed in

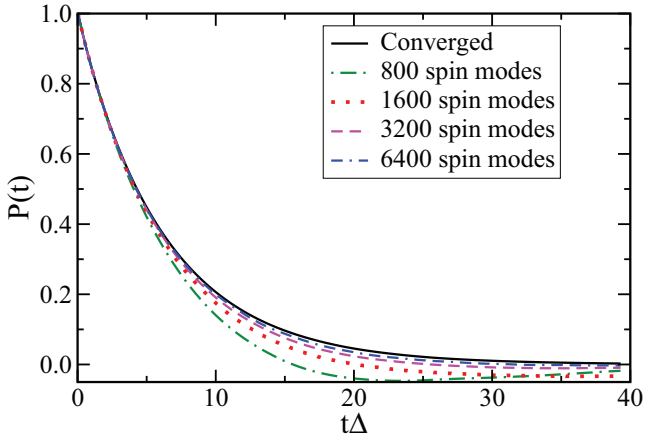

FIG. 3. Time-dependent population difference for a spin bath with a characteristic frequency $\omega_c/\Delta = 40$ and zero temperature. The Kondo parameter is $\alpha = 0.5$.

terms of the convergence criteria in a typical ML-MCTDH simulation. This accuracy is particularly important since $\alpha = 0.5$ defines the approximate coherent-incoherent transition boundary in the scaling limit $\omega_c/\Delta \to \infty$. Lastly, when the Kondo parameter is increased to $\alpha = 0.75$, as many as 6400 bath spin modes are required to converge the result within the time scale shown in Fig. 2(c). The corresponding spin-boson model, on the other hand, only requires 500 modes to achieve the same accuracy. This suggests that in the strong coupling regime of the nonadiabatic limit, many more bath spin modes are required to dilute the coupling strength in order to achieve convergence in the dynamics and to the linear response limit. The situation is worse when the time scale of the bath further increases, as shown in Fig. 3 with $\omega_c/\Delta = 40$. Here, even for $\alpha = 0.5$, a bath of 6400 spin modes are not sufficient and the accurate result is obtained with 9600 bath spin modes. Under these circumstances it is easier to carry out the ML-MCTDH study on the mapped spin-boson model, for which less than a thousand discrete modes provide converged dynamical results.

The above numerical tests show that although the spin-spin-bath model can be mapped onto the familiar spin-boson model in the linear response limit, many degrees of freedom are required to fulfill the practical requirement. Thus, caution needs to be taken in the actual modeling procedure to verify whether linear response is a good approximation. It should also be mentioned that the model discussed here satisfies, by construction, the requirement of linear response because of the continuous spectral density function employed. This is not the case if the spectral density contains some discrete terms, i.e., some intrinsically nonlinear degrees of freedom just as the intramolecular modes in electron transfer process. Such models can be found in realistic applications and will be the subject of future work.

B. The role of temperature in the coherent-incoherent transition

It is generally believed that for an open system the role of a heat bath is to provide a dissipative environment. At higher

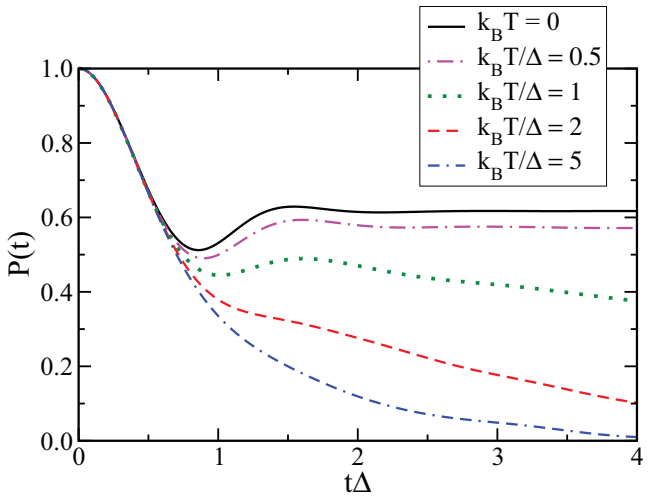

FIG. 4. Time-dependent population difference for a spin bath with a characteristic frequency $\omega_c/\Delta = 1$ and Kondo parameter $\alpha = 10$.

temperatures there are more bath states participating in the overall dynamics, which provides more effective quenching to quantum effects such as the coherence an isolated system exhibits. However, some previous studies show that for the spin-spin-bath model increasing the temperature may slightly enhance the coherence of the central two-level subsystem in the nonadiabatic regime,[37,38] a result somewhat counter-intuitive. Another study,[39] on the other hand, concludes that the coherent-incoherent boundary is independent of the temperature. Here, we use the numerically exact ML-MCTDH method to address this discrepancy.

Since a coherent to incoherent transition depends on the physical regime, we first show a result where there is no clear time scale separation between the bath and the subsystem, $\omega_c/\Delta = 1$. Figure 4 illustrates the effect of temperature for $\alpha = 10$ [i.e., the parameters used in Fig. 1(b)]. At zero temperature, $P(t)$ first displays a transient coherent motion, and then reaches its stationary value. For a large coupling strength in an adiabatic (or intermediate between adiabatic and nonadiabatic) regime, the barrier along the adiabatic double-well potential can be high enough to induce localization of the population, such as observed here. As the temperature of the spin bath is raised, more energy may be available to assist the subsystem get out of the trap. Furthermore, as shown in Eq. (3.1), the linear response mapped effective spectral density becomes smaller in magnitude at higher temperatures, thus lowering the double-well's barrier height. Both effects will promote the system moving from its localized state, and this is indeed what we have found in the simulation. As depicted in Fig. 4, increasing the temperature induces a faster decay to the delocalized population distribution for the central spin. The resulting time-dependent dynamics of $P(t)$ becomes less coherent.

The above result is informative but beyond many approximate theories that require a well-defined time scale separation between the subsystem and the bath. Let us now turn to the nonadiabatic regime, which is the subject of the previous approximate theoretical treatment and which raises some disagreement in conclusions. Figure 5 is an example of the nonadiabatic regime ($\omega_c/\Delta = 6$) that has been studied by the path

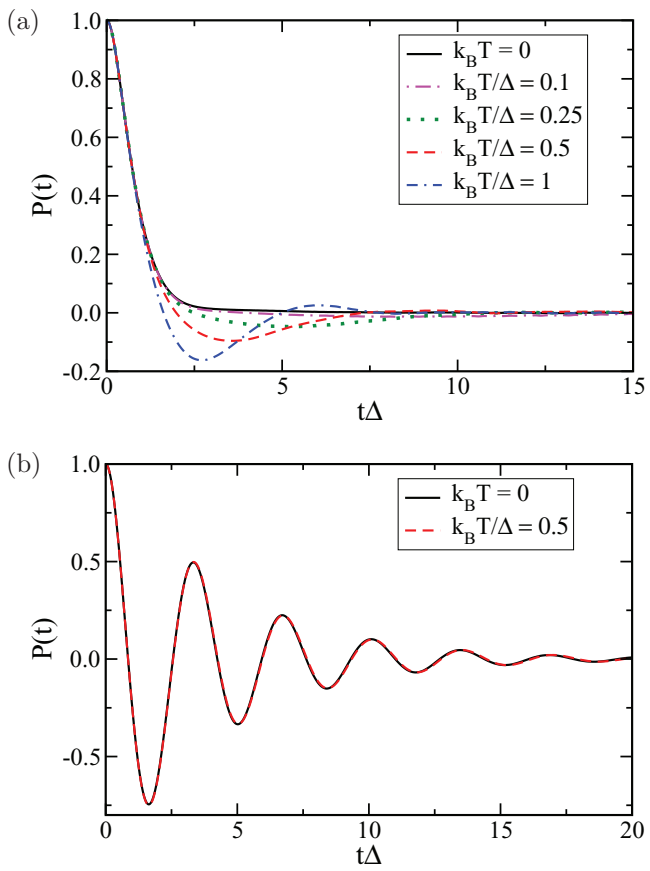

FIG. 5. Time-dependent population difference for a spin bath with a characteristic frequency $\omega_c/\Delta = 6$ and Kondo parameters: (a) $\alpha = 0.5$, (b) $\alpha = 0.1$.

integral method.[38] Figure 5(a) shows $P(t)$ for several temperatures with the Kondo parameter $\alpha = 0.5$. At zero temperature, $P(t)$ exhibits a clear incoherent decay to its final stationary value of $P = 0$. However, even with a little increase in the bath temperature, $k_BT/\Delta = 0.1$, $P(t)$ becomes slightly negative in its transient dynamics and slowly recovers to its stationary value in the long time limit. A further increase in temperature induces stronger coherent motion with a shorter period. Therefore, temperature plays a positive role here of inducing the coherence. As a comparison, for a weaker system-bath coupling strength, $\alpha = 0.1$, the population dynamics is already coherent at zero temperature. Figure 5(b) shows that increasing the bath temperature within a similar range does not have significant impact on $P(t)$. Finally, it is noted that Fig. 5 agrees with the previous path integral results for $k_BT/\Delta = 0.5$.

Thus, our simulation suggests that increasing the bath temperature promote coherent dynamics of the central two-level subsystem, a result in agreement with the previous work of Shao and Hänggi[37] and Forsythe and Makri.[38] To further illustrate this point, Fig. 6 shows $P(t)$ versus bath temperature for $\omega_c/\Delta = 10$ and three Kondo parameters: $\alpha = 0.5$, $\alpha = 0.6$, and $\alpha = 0.75$. From NIBA analysis in the scaling limit ($\omega_c \to \infty$), $\alpha = 0.5$ is the approximate boundary for the coherent-incoherent transition at zero temperature, i.e., for $\alpha > 0.5$ the dynamics of $P(t)$ at zero temperature is characterized by an incoherent relaxation. This is confirmed by the

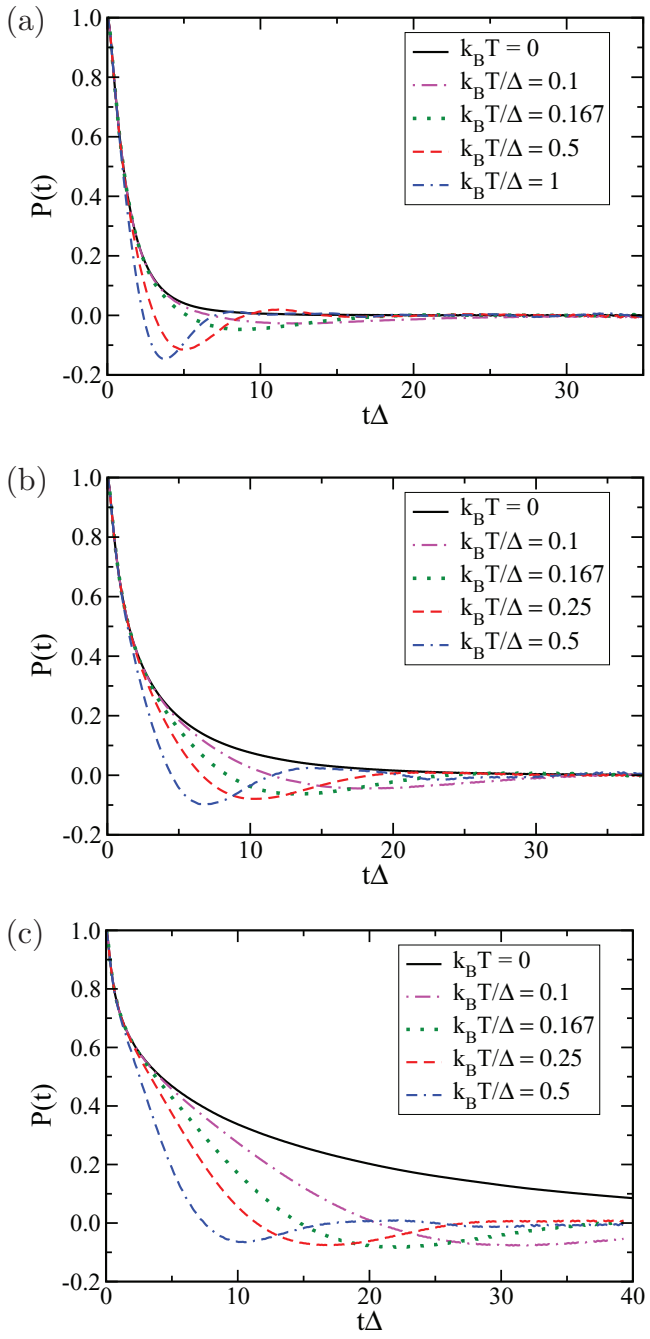

FIG. 6. Time-dependent population difference for a spin bath with a characteristic frequency $\omega_c/\Delta = 10$ and Kondo parameters: (a) $\alpha = 0.5$, (b) $\alpha = 0.6$, (c) $\alpha = 0.75$.

results shown in Fig. 6. However, a striking feature that exists in $P(t)$ for all the three Kondo parameters is that even with a low bath temperature, $k_BT/\Delta = 0.1$, $P(t)$ becomes slightly negative (and thus coherent) in its transient dynamics and then slowly comes back to its stationary value of $P = 0$. This is true even for a relatively large Kondo parameter, $\alpha = 0.75$ in Fig. 6(c). Another feature shown in Fig. 6 is that the transient coherent period becomes longer as the Kondo parameter increases. Calculations for other Kondo parameters in this range suggest similar behavior.

In general, increasing temperature of the bath means that more excitations are available and thus fluctuations becomes stronger, which is detrimental to quantum coherence the system can display. For the spin-spin-bath model considered in this paper, however, the argument is not an accurate description of the true physical situation because the number of the states for each bath spin is limited to two. Nevertheless, an increase in temperature (from zero K) in the nonadiabatic regime brings about two competing effects. On one hand, the heat bath has more energy/excitations and may quench the coherent dynamics more effectively. On the other hand, the effective spectral density for the mapped spin-boson model, Eq. (3.1), has a smaller magnitude when the temperature is higher. This renders weaker coupling to the central spin and results in more coherent dynamics of the subsystem. For lower temperatures our simulation indicates that the second effect dominates. This is surprising if one plots the effective spectral density of Eq. (3.1), for it is nearly identical to, or with an exponentially small difference from the spectral density at zero K. However, upon closer examination, it is found that the low frequency end of the spectral density is most affected in the effective spectral density. In the nonadiabatic regime it is this part that couples more effectively to the two-level subsystem. Therefore, reducing this part when increasing the bath temperature will reduce the effective system-coupling strength and thus induce more coherence in the dynamics of $P(t)$.

C. The coherent-incoherent boundary at low temperatures

The above results suggest that upon increasing the bath temperature the coherent-incoherent boundary is shifted to the larger coupling strength. The simulation results shown in Fig. 6 is consistent with the previous NIBA calculation[38] that even at a very low temperatures the coherent-incoherent boundary is located approximately at $\alpha = 0.75$ or even larger. However, at zero temperature the spin-spin-bath model has identical reduced dynamics as the spin-boson model. Since for the latter the coherent-incoherent transition is at $\alpha = 0.5$ in the scaling limit, Ref. 39 raises some doubts on the phase diagram obtained from the NIBA calculation.[38] To answer this question we perform the ML-MCTDH simulation at zero temperature to locate the coherent-incoherent boundary.

Certain ambiguity exists in defining the coherent to incoherent transition. For an unbiased spin subsystem, we use the definition of Ref. 38 that if $P(t)$ has a small negative transient lobe, it is called coherent. The converged ML-MCTDH calculations can have a resolution of $P(t) = -0.005$ or better. As shown in Fig. 7, this transition occurs at approximately $\alpha = 0.46$ [i.e., at and above which there is no negative value in transient $P(t)$] for all three characteristic frequencies of the bath, though the time scales for the transient dynamics of $P(t)$ are different. Of course, one may argue that in the scaling limit only $\alpha = 0.5$ has a single exponential decay in $P(t)$. For a slightly smaller α depicted in Fig. 7, $P(t)$ may be fitted to a damped oscillation although it does not become negative. This, however, will only change the transition boundary slightly. Furthermore, when α becomes larger than 0.5 the dynamics of $P(t)$ involves multiple time scales and cannot be described by a single exponential decay either.[55] In this sense

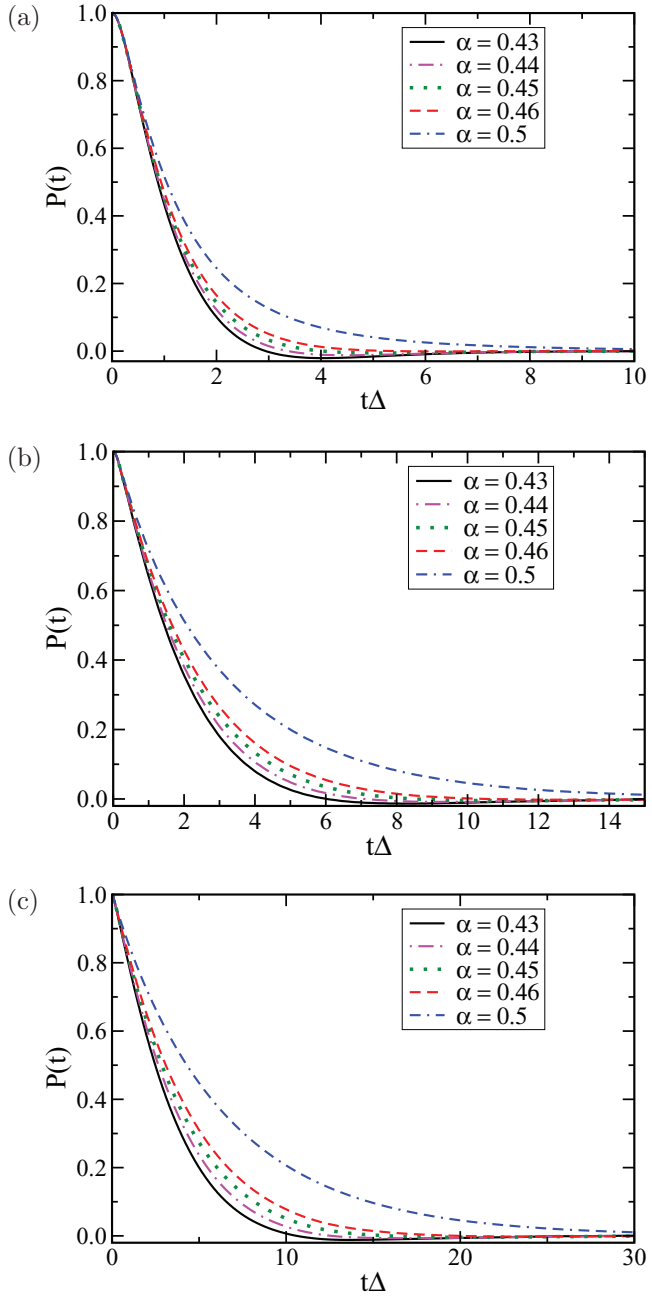

FIG. 7. Time-dependent population difference for a spin bath at zero temperature. The characteristic frequencies are: (a) $\omega_c/\Delta = 10$, (b) $\omega_c/\Delta = 20$, (c) $\omega_c/\Delta = 40$.

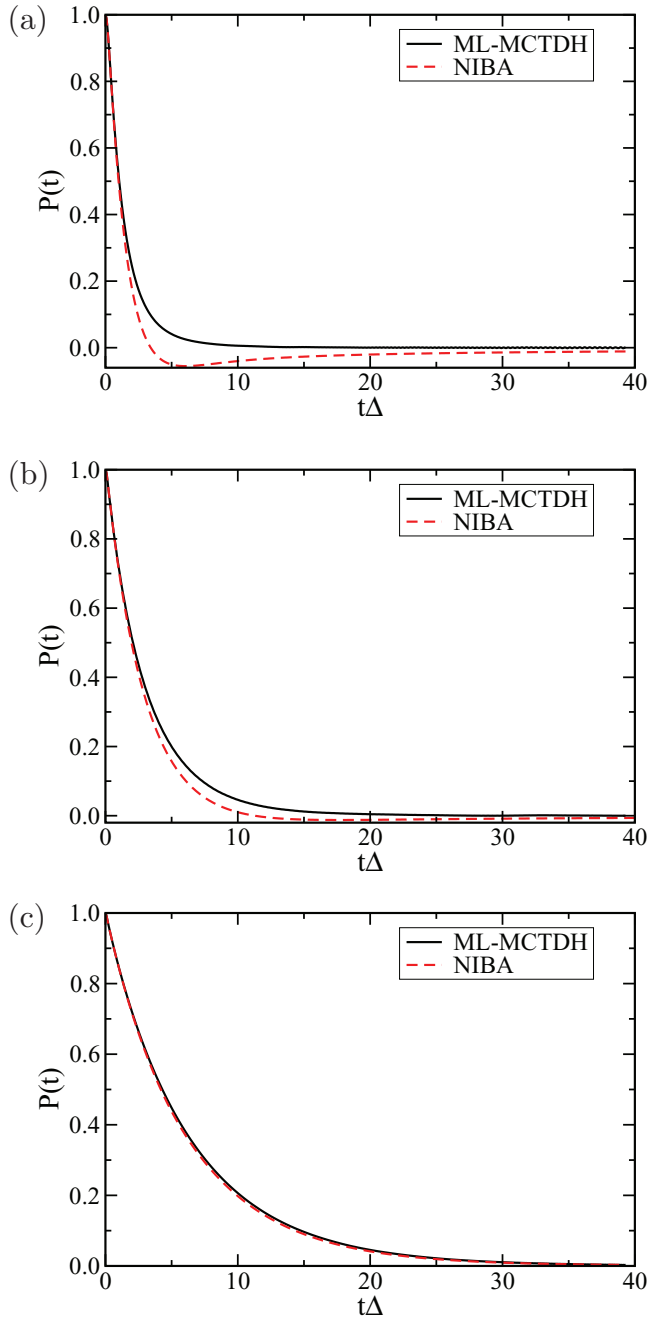

FIG. 8. Comparison of the time-dependent population between the ML-MCTDH and NIBA results. The bath temperature is zero and the Kondo parameter is $\alpha = 0.5$. The characteristic frequencies are: (a) $\omega_c/\Delta = 10$, (b) $\omega_c/\Delta = 20$, (c) $\omega_c/\Delta = 40$.

a single exponential decay may also be an inappropriate separation between the coherent and incoherent dynamics. Therefore, we conclude that according to our ML-MCTDH simulation the coherent-incoherent boundary at zero temperature is located at α slightly less than 0.5.

With respect to the accuracy of the NIBA approach for predicting the coherent-incoherent boundary, Fig. 8 shows the comparison between the ML-MCTDH simulation and the NIBA calculation at zero temperature and a Kondo parameter $\alpha = 0.5$. It is seen that for a (relatively) smaller characteristic frequency $\omega/\Delta = 10$, there are some small differences between the NIBA and the exact result. In particular, $P(t)$ obtained from NIBA exhibits a quenched coherent motion whereas the ML-MCTDH result does not. Thus, NIBA or similar perturbation theory would predict the coherent-incoherent boundary to be located at $\alpha > 0.5$ at zero temperature. On the other hand, exact results show that this boundary resides at $\alpha < 0.5$. As the characteristic frequency increases, NIBA becomes more accurate and eventually exact in the scaling limit, in which the coherent-incoherent boundary agrees with the exact result.

Figure 9 further illustrates the performance of NIBA at zero temperature for a bath characteristic frequency of $\omega/\Delta = 10$. It demonstrates that NIBA calculations deviate

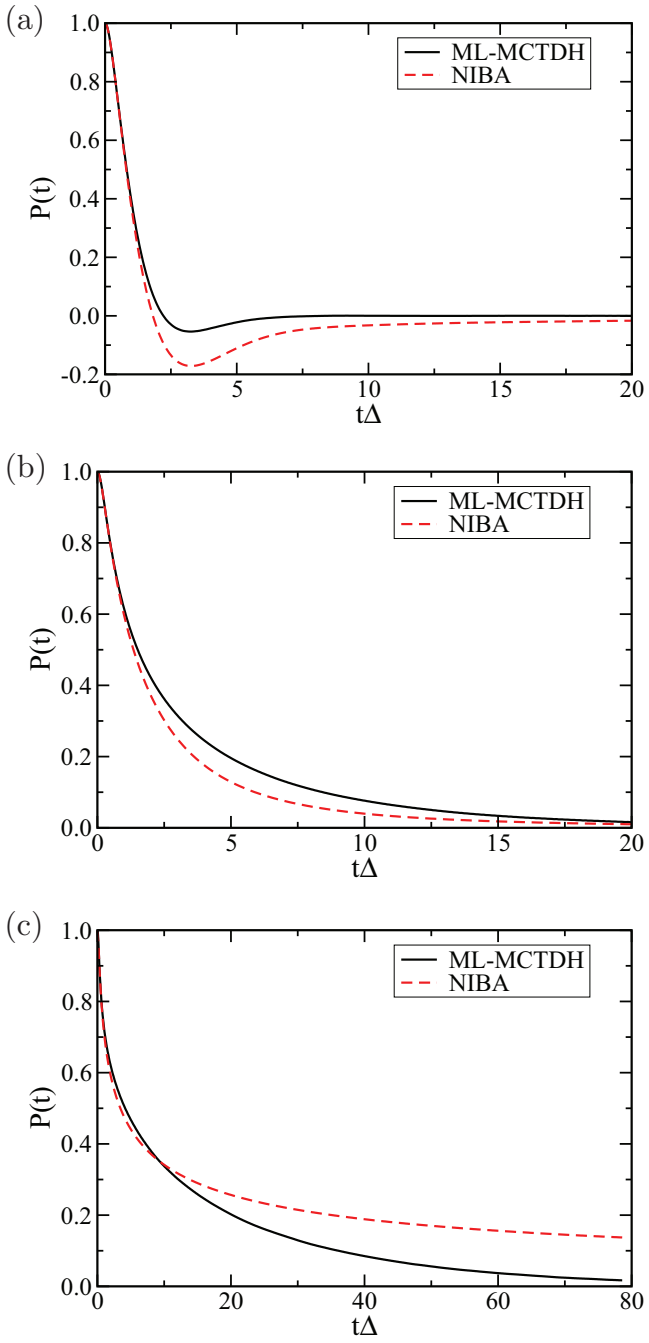

FIG. 9. Comparison of the time-dependent population between the ML-MCTDH and NIBA results. The bath temperature is zero and the characteristic frequency is $\omega_c/\Delta = 10$. The Kondo parameters are: (a) $\alpha = 0.4$, (b) $\alpha = 0.6$, (c) $\alpha = 0.75$.

from the exact results, especially in the stronger coupling regime. However, combining Figs. 8 and 9, NIBA captures the coherent-incoherent transition at a qualitative level even though its predicted $P(t)$ is not accurate. At higher temperatures, NIBA is expected have a better performance.

IV. CONCLUDING REMARKS

Thus, our ML-MCTDH simulation reveals that for the spin-spin-bath model increasing the bath temperature will enhance the coherence of $P(t)$ in the nonadiabatic regime, a result consistent with the previous approximate theories.[37,38] The exact coherent-incoherent boundary is slightly less than $\alpha = 0.5$ at zero temperature. The boundary is shifted to the stronger coupling regime at $\alpha = 0.7$–0.8 even for a very low (but nonzero) temperature, e.g., $k_BT/\Delta = 0.1$. Although increasing the temperature may either enhance the bath excitation and thus favors decoherence, or reduce the coupling between the bath and the two-level subsystem as demonstrated in its effective spectral density in the mapped spin-boson model, our simulation suggests the latter dominates in the low temperature regime.

Our simulation also shows that a different behavior may be observed if the model is in the adiabatic regime or the intermediate regime between the adiabatic and nonadiabatic limit, e.g., Fig. 4. In such a situation increasing the temperature may break the localization at zero temperature and also quench the transient coherence. This finding shows the complex interplay between the coherent-incoherent transition and the physical regime the system belongs to. It also suggests that caution must be taken when using an approximate perturbation theory to quantify such properties.

In this work, we have assumed a continuous spectral density for the spin-spin-bath model as used in the previous studies. This implies that the model obeys the linear response requirement in the infinite bath modes limit, and thus can be mapped to the more familiar spin-boson model. This may not be the case for realistic physical problems, e.g., a spin glass. Thereby, some intrinsically anharmonic contributions may be important. The ML-MCTDH methodology is well suited for studying such problems and will be applied in such future studies.

ACKNOWLEDGMENTS

This work was supported by the National Science Foundation (NSF) CHE-1012479 (H.W.) and used resources of the National Energy Research Scientific Computing Center, which is supported by the Office of Science of the (U.S.) Department of Energy (DOE) under Contract No. DE-AC02-05CH11231. J.S. acknowledges the support from the National Natural Science Foundation of China (NNSFC) (Grant No. 91027013) and the 973 program of the Ministry of Science and Technology of China (2011CB808502).

[1] A. O. Caldeira and A. J. Leggett, Ann. Phys. (NY) **149**, 374 (1983).
[2] A. O. Caldeira and A. J. Leggett, Ann. Phys. (NY) **153**, 445(E) (1983).
[3] A. J. Leggett, S. Chakravarty, A. T. Dorsey, M. P. A. Fisher, A. Garg, and W. Zwerger, Rev. Mod. Phys. **59**, 1 (1987).
[4] U. Weiss, *Quantum Dissipative Systems*, 2nd ed. (World Scientific, Singapore, 1999).
[5] C. Aslangul, N. Pottier, and D. Saint-James, J. Phys. **47**, 1657 (1986).
[6] R. A. Harris and R. Silbey, J. Chem. Phys. **78**, 7330 (1983).
[7] C. Meier and D. J. Tannor, J. Chem. Phys. **111**, 3365 (1999).
[8] L. Hartmann, I. Goychuk, M. Grifoni, and P. Hänggi, Phys. Rev. E **61**, 4687 (2000).
[9] L. Zusman, Chem. Phys. **49**, 295 (1980).
[10] A. Garg, J. Onuchic, and V. Ambegaokar, J. Chem. Phys. **83**, 4491 (1985).
[11] D. Y. Yang and R. I. Cukier, J. Chem. Phys. **91**, 281 (1989).
[12] Y. Jung, R. J. Silbey, and J. Cao, J. Phys. Chem. A **103**, 9460 (1999).
[13] H. Lehle and J. Ankerhold, J. Chem. Phys. **120**, 1436 (2004).
[14] C. Zhang, M.-H. Du, H.-P. Cheng, X.-G. Zhang, A. Roitberg, and J. L. Krause, Phys. Rev. Lett. **92**, 158301 (2004).

[15]X. Sun, H. Wang, and W. H. Miller, J. Chem. Phys. **109**, 7064 (1998).
[16]G. Stock and U. Müller, J. Chem. Phys. **111**, 65 (1999).
[17]H. Wang, X. Song, D. Chandler, and W. H. Miller, J. Chem. Phys. **110**, 4828 (1999).
[18]G. Stock and M. Thoss, Adv. Chem. Phys. **131**, 243 (2005).
[19]E. Martin-Fierro and E. Pollak, J. Chem. Phys. **126**, 164108 (2007).
[20]R. Egger and C. H. Mak, Phys. Rev. B **50**, 15210 (1994).
[21]N. Makri and D. E. Makarov, J. Chem. Phys. **102**, 4600 (1995).
[22]E. Sim and N. Makri, J. Phys. Chem. **101**, 5446 (1997).
[23]L. Mühlbacher and R. Egger, J. Chem. Phys. **118**, 179 (2003).
[24]R. Bulla, N.-G. Tong, and M. Vojta, Phys. Rev. Lett. **91**, 170601 (2003).
[25]F. B. Anders and A. Schiller, Phys. Rev. B **74**, 245113 (2006).
[26]F. Anders, R. Bulla, and M. Voitja, Phys. Rev. Lett. **98**, 210402 (2007).
[27]Y. Zhou, Y. Yan, and J. Shao, Europhys. Lett. **72**, 334 (2005).
[28]Y. Zhou and J. Shao, J. Chem. Phys. **128**, 034106 (2008).
[29]H. Wang, M. Thoss, and W. Miller, J. Chem. Phys. **115**, 2979 (2001).
[30]M. Thoss, H. Wang, and W. H. Miller, J. Chem. Phys. **115**, 2991 (2001).
[31]H. Wang and M. Thoss, Isr. J. Chem. **42**, 167 (2002).
[32]R. A. Marcus and N. Sutin, Biochim. Biophys. Acta **811**, 265 (1985).
[33]A. Suárez and R. Silbey, J. Chem. Phys. **95**, 9115 (1991).
[34]U. Weiss, H. Grabert, and S. Linkwitz, J. Low Temp. Phys. **68**, 213 (1987).
[35]A. S. Davydov, *Quantum Mechanics*, 2nd ed. (Pergamon, Oxford, 1976), p. 440.
[36]A. O. Caldeira, A. H. C. Neto, and T. O. de Carvalho, Phys. Rev. B **48**, 13974 (1993).
[37]J. Shao and P. Hänggi, Phys. Rev. Lett. **81**, 5710 (1998).
[38]K. M. Forsythe and N. Makri, Phys. Rev. B **60**, 972 (1999).
[39]Z. Lü and H. Zheng, J. Chem. Phys. **131**, 134503 (2009).
[40]H. Wang and M. Thoss, J. Chem. Phys. **119**, 1289 (2003).
[41]N. Makri, J. Phys. Chem. B **103**, 2823 (1999).
[42]H. Wang and M. Thoss, J. Phys. Chem. A **111**, 10369 (2007).
[43]H. Wang and M. Thoss, J. Chem. Phys. **124**, 034114 (2006).
[44]H. Wang, D. Skinner, and M. Thoss, J. Chem. Phys. **125**, 174502 (2006).
[45]H.-D. Meyer, U. Manthe, and L. S. Cederbaum, Chem. Phys. Lett. **165**, 73 (1990).
[46]U. Manthe, H.-D. Meyer, and L. S. Cederbaum, J. Chem. Phys. **97**, 3199 (1992).
[47]M. H. Beck, A. Jäckle, G. A. Worth, and H.-D. Meyer, Phys. Rep. **324**, 1 (2000).
[48]H.-D. Meyer and G. A. Worth, Theor. Chem. Acc. **109**, 251 (2003).
[49]M. Thoss, I. Kondov, and H. Wang, Chem. Phys. **304**, 169 (2004).
[50]M. Thoss and H. Wang, Chem. Phys. **322**, 210 (2006).
[51]I. R. Craig, H. Wang, and M. Thoss, J. Chem. Phys. **127**, 144503 (2007).
[52]H. Wang and M. Thoss, Chem. Phys. **347**, 139 (2008).
[53]K. A. Velizhanin, H. Wang, and M. Thoss, Chem. Phys. Lett. **460**, 325 (2008).
[54]J. Li, M. Nilsing, I. Kondov, H. Wang, P. Persson, S. Lunell, and M. Thoss, J. Phys. Chem. C **112**, 12326 (2008).
[55]H. Wang and M. Thoss, New J. Phys. **10**, 115005 (2008).
[56]H. Wang and M. Thoss, J. Chem. Phys. **131**, 024114 (2009).
[57]K. A. Velizhanin and H. Wang, J. Chem. Phys. **131**, 094109 (2009).
[58]H. Wang and M. Thoss, Chem. Phys. **370**, 78 (2010).
[59]I. Craig, M. Thoss, and H. Wang, J. Chem. Phys. **135**, 064504 (2011).
[60]H. Wang and M. Thoss, J. Phys. Chem. A **107**, 2126 (2003).